Published in final edited form as:
Mol Microbiol. 2011 March ; 79(5): 1182–1193. doi:10.1111/j.1365-2958.2011.07540.x.

NifB and NifEN protein levels are regulated by ClpX2 under nitrogen fixation conditions in *Azotobacter vinelandii*

Giselle Martínez-Noël[1,†], **Leonardo Curatti**[2,*,†], **Jose A. Hernandez**[3], and **Luis M. Rubio**[1]

[1] Fundación IMDEA Energía, Centro de Biotecnología y Genómica de Plantas, Campus Montegancedo, Pozuelo de Alarcón 28223 Madrid, Spain

[2] Centro de Investigaciones Biológicas, FIBA, Mar del Plata, Argentina and Centro de Estudios de Biodiversidad y Biotecnología de Mar del Plata, CONICET, Argentina

[3] Department of Biochemistry, AZCOM, Midwestern University, Glendale, AZ 85308, USA

Summary

The major part of biological nitrogen fixation is catalyzed by the molybdenum nitrogenase that carries at its active site the iron and molybdenum cofactor (FeMo-co). The nitrogen fixation (*nif*) genes required for the biosynthesis of FeMo-co are derepressed in the absence of a source of fixed nitrogen. The *nifB* gene product is remarkable because it assembles NifB-co, a complex cluster proposed to have a [6Fe-9S-X] composition, from simpler [Fe-S] clusters common to other metabolic pathways. NifB-co is a common intermediate of the biosyntheses of the cofactors present in the molybdenum, vanadium and iron nitrogenases. In this work, the expression of the *Azotobacter vinelandii nifB* gene was uncoupled from its natural *nif*-regulation to show that NifB protein levels are lower in cells growing diazotrophically than in cells growing at the expense of ammonium. *A. vinelandii* carries a duplicated copy of the ATPase component of the ubiquitous ClpXP protease (ClpX2) which is induced under nitrogen fixing conditions. Inactivation of *clpX2* resulted in the accumulation of NifB and NifEN and a defect in diazotrophic growth, especially when iron was in short supply. Mutations in *nifE, nifN and nifX* and in *nifA* also affected NifB accumulation, suggesting that NifB susceptibility to degradation might vary during its catalytic cycle.

Introduction

The major part of biological nitrogen fixation is catalyzed by the molybdenum nitrogenase, although some nitrogen-fixing bacteria additionally contain alternative vanadium or iron-only nitrogenases that are expressed when molybdenum is not available (Eady, 1996). The molybdenum nitrogenase is composed of two proteins that can be separately purified: dinitrogenase and dinitrogenase reductase. Dinitrogenase, is a 220-to 240-kDa tetramer of the *nifD* and *nifK* gene products that contains two pairs of two complex metalloclusters. Dinitrogenase reductase, is a 60-kDa dimer of the product of the *nifH* gene, which contains a single [4Fe-4S] cluster and two Mg-ATP binding sites and is the obligate electron donor to the molybdenum dinitrogenase. The molybdenum nitrogenase carries at its active site a complex iron-molybdenum cofactor (FeMo-co) composed of seven Fe, nine S, one Mo, one

*Corresponding author: lcuratti@fiba.org.ar.
†These authors contributed equally to this work

Supporting information
Additional supporting information may be found in the online version of this article.

homocitrate, and one light atom proposed to be C, N or O (Einsle *et al.*, 2002, Lukoyanov *et al.*, 2007).

Genetic and biochemical studies in free-living diazotrophic bacteria, mainly *Azotobacter vinelandii* and *Klebsiella pneumoniae*, have shown that a number of nitrogen fixation (*nif*) genes are involved in FeMo-co biosynthesis and the formation of an active nitrogenase enzyme. Among them, *nifB* has been shown to be crucial for global nitrogen fixation because its product, the SAM-radical enzyme NifB, catalyzes the assembly of NifB-co, which is a common precursor for the biosyntheses of FeMo-co and the analogous iron-vanadium (FeV) and iron-only (FeFe) cofactors, carried by the vanadium and the iron-only nitrogenases, respectively (Bishop and Joerger, 1990; Curatti *et al.*, 2006 and 2007).

NifB-co has been proposed to comprise the [6Fe-9S-X] core of FeMo-co (George *et al.*, 2008). Maturation of NifB-co into FeMo-co requires its transfer to the NifEN scaffold protein, onto which additional Fe, the Mo atom, and homocitrate are incorporated into the precursor to generate FeMo-co in a series of reactions, some of which require NifH, Mg-ATP and reductant (see Rubio and Ludden, 2008 for a review).

Because NifB catalyzes the first committed step in dinitrogenase cofactor biosynthesis, cellular NifB levels and activity are expected to be tightly regulated. The expression of *nifB* has been shown to be under the regulation of the transcriptional activators from the three nitrogenase systems, NifA, VnfA and AnfA (Drummond *et al.*, 1996). However, the existence of additional mechanisms regulating the levels of NifB, is not known.

In *A. vinelandii* and other diazotrophs, duplicated copies of housekeeping genes have acquired *nif* regulation to boost or gain specific functions during nitrogen fixation. Two well-studied examples are the *nifUS* genes, which are homologous to the house keeping *iscUS* genes, and the *rnf1* gene cluster, which is homologous to the *rnf2* and to the NADH-ubiquinone oxidoreductase gene clusters. NifU and NifS appear to boost the biosynthesis of [Fe-S] clusters for nitrogenase proteins (Dos Santos *et al*., 2007, Zhao *et al*., 2007), whereas *rnf1* has acquired roles in modulation of *nif* genes expression and in NifH maturation (Curatti *et al*., 2005).

The *A. vinelandii* genome carries two ClpX-like encoding sequences in the open reading frames Avin23580 and Avin01700. Avin23580 might represent the house keeping *clpX* copy since it is located in a similar genetic context as *clpX* genes from non-diazotrophic bacteria and its product exhibits higher similarity to the ClpX subunit of ClpXP proteases. ClpXP is an ATP-dependent protease that is widespread in nature and shares a basic mechanism with the proteasome of eukaryotic organisms (Dougan *et al.*, 2002; Zolkiewski, 2006). The ClpX component is a hexameric AAA^{+}ATPase responsible for substrate recognition, unfolding, and translocation into ClpP, a serine peptidase. ClpX can also act independently to dismantle multimers and remodel proteins (Kim *et al*., 2000).

On the other hand, Avin01700, hereafter denominated as *clpX2*, is located between the *nifM* and *nifF* genes in the major *nif* cluster in *A. vinelandii* (Setubal *et al.*, 2009). Homologs to *clpX2* have also been found within *nif* gene clusters in other diazotrophs. ClpX2 is not essential for nitrogen fixation since disruption of the *clpx2* gene in *A. vinelandii* resulted in a Nif+ phenotype (Jacobson *et al.*, 1989). On the other hand, transposon mutagenesis of a house-keeping type *clpX* in *Azospirillum brasilense* resulted in a 3-fold increase in nitrogenase activity among other pleiotropic effects (Rodriguez *et al.*, 2006).

Here we demonstrate that the *A. vinelandii* ClpX2 protein is part of a nitrogen source-dependent regulatory mechanism that controls the cellular levels of NifB and NifEN proteins by means of protein degradation. Thus, a regulatory layer superimposed on

transcriptional control exists in the model diazotrophic organism *A. vinelandii* to fine tune nitrogenase cofactor biosynthesis.

Results

NifB stability is influenced by the nitrogen source

As part of our studies to understand the function and regulation of NifB in *A. vinelandii*, we constructed an *A. vinelandii* conditional Nif-defective strain (UW233) in which the original *nifB* gene had been replaced by a *gst::nifB* chimeric gene under the control of an IPTG-inducible promoter (Fig. 1A). UW233 was unable to grow diazotrophically unless the medium was supplemented with IPTG, as expected (Fig. S1). The accumulation of GST-NifB in UW233, upon IPTG induction, was verified by immunoblots developed with antibodies to NifB (Fig. 1B). This strategy allowed controlling GST-NifB accumulation in the cells in response to the concentration of IPTG added to the medium (Fig. 1C).

Induction of *gst::nifB* expression by IPTG addition showed that GST-NifB accumulated to higher levels in *A. vinelandii* cells growing with ammonium as nitrogen source than in cells growing diazotrophically (Fig. 2A). To determine whether this difference in GST-NifB accumulation was due to changes in NifB stability, we investigated the changes in GST-NifB degradation rates according to the nitrogen source used by the cells. UW233 cells growing with ammonium as nitrogen source were loaded with GST-NifB by supplementing the medium with 10 mM IPTG for 2 h. UW233 cells were then collected, washed with medium lacking ammonium and IPTG, and then incubated in fresh medium lacking or containing ammonium. As shown in Fig. 2B, UW233 cells were able to grow diazotrophically at the expense of the accumulated GST-NifB protein. Immunoblot analysis showed that the degradation of GST-NifB was much slower in cells growing with ammonium as nitrogen source than in those growing diazotrophically (Fig. 2C). Depletion of GST-NifB was more pronounced by the time dinitrogenase polypeptides (NifDK) started to accumulate (Fig. 2C) and was almost undetectable 4 h after the onset of nitrogenase derepressing conditions (Fig. 2D).

Similarly, extracts obtained from *A. vinelandii* UW140 (Δ*nifB*) cells grown under diazotrophic conditions were shown to promote the *in vitro* degradation of GST-NifB present in extracts of IPTG-induced ammonium-grown UW233 cells. *In vitro* GST-NifB degradation rates were stimulated by the addition of ATP to the reaction mixtures (Fig. S2). Altogether, these results indicate that a proteolytic system involved in NifB degradation is induced under diazotrophic growth conditions.

NifB stability is influenced by mutations in nifENX and nifA

We had previously observed that NifB accumulated to a larger extent in a mutant strain lacking *nifENX* (UW235) than in the wild-type strain (Fig. S3). Uncoupling *nifB* expression from its natural *nif* regulation did not restore the wild-type phenotype (Fig. 2A), suggesting that the accumulation of NifB observed in the cells from Δ*nifENX* strains was due to increased NifB stability rather than higher *nifB* transcriptional rates. Moreover, the Δ*nifENX* strain exhibited low GST-NifB degradation rates regardless of the presence or absence of ammonium in the medium (Fig. 3B).

The stability of GST-NifB was also investigated in the Δ*nifA* genetic background, in which expression of most (or all) major *nif* genes is abolished. Surprisingly, GST-NifB became more unstable in the absence of NifA, especially under diazotrophic growth conditions (Fig. 3C), which suggested that the nitrogen source-dependent proteolytic factor involved in NifB degradation was not the product of a NifA-dependent *nif* gene.

The A. vinelandii genome contains two copies of clpX-like genes

The phylogenetic analysis in Fig. 4A shows that, while the product of the *A. vinelandii* Avin23580 gene (*clpX*) is most similar to ClpX proteins found in diverse non-diazotrophic microorganisms, the product of Avin01700 (*clpX2*) is more similar to ClpX proteins present in other diazotrophs such as *Pseudomonas stutzeri*. In addition, both in *A. vinelandii* and in *P. stutzeri*, the *clpX2* genes are located among characterized *nif* genes and, in the case of *A. vinelandii*, it was previously denominated as *orf9*.

The predicted ClpX2 protein from *A. vinelandii* exhibited 50% sequence similarity to the *Escherichia coli* ClpX ortholog and contained the conserved the sequence motifs known to be essential to protease activity in *E. coli* ClpX (Fig. 4B). However, the C-terminal region of *A. vinelandii* ClpX2 was especially distinct from the described ClpX proteins.

A. vinelandii clpX2 expression is regulated by the nitrogen source

To study the expression of *clpX2*, *A. vinelandii* strains containing chromosomal transcriptional fusions between the sequence upstream of *clpX2* and the *lacZ* reporter gene were generated (Fig. 5A). β-galactosidase activity assays revealed that ammonium removal from the medium increased *clpX2* gene expression by 3.5-fold in a period of 3 h (Fig. 5B). To ascertain whether such increase was dependent on *nifA*, β-galactosidase activity was determined in a *clpX2::lacZ* reporter strain carrying a *ΔnifA* mutation (Fig. 5A). Interestingly, induction of *clpX2* expression in the absence of ammonium appeared not to require NifA (Fig. 5B). Moreover, *clpX2* expression is apparently higher in the absence of NifA. The molecular basis of this effect is not currently understood. Expression of *clpX2* according to the nitrogen source and the existence of an mRNA species comprising at least part of *nifM* and *clpX2* have been confirmed by semiquantitative RT-PCR (data not shown).

ClpX2 is involved in the regulation of NifB and NifEN levels

To investigate the possible participation of *clpX2* in the nitrogen source-dependent proteolytic system responsible for NifB degradation, a mutant strain (UW322) bearing an in-frame deletion of most of the *clpX2* gene was generated (Fig. 6A). Immunoblot analyses showed that, 3 h after ammonium removal from the medium, the NifB and NifEN polypeptide levels were significantly higher in the Δ*clpX2* mutant strain than in the wild-type strain, while NifDK, NifH, NifX and NafY polypeptide levels remained almost unchanged (Fig. 6B). Relative NifB levels were 3-fold higher, whereas the difference in NifEN accumulation between the Δ*clpX2* and the wild-type strains was even more remarkable, suggesting a participation of ClpX2 in NifB and NifEN polypeptide turnover.

The *in vivo* decay of NifB polypeptides was analyzed by using *A. vinelandii* cells treated with spectinomycin 3 h after derepression of *nif* gene expression in order to stop protein synthesis. Fig. 7 shows that the degradation rate of NifB polypeptides *in vivo* was slower in the Δ*clpX2* mutant than in the wild-type strain. In contrast, the degradation rates of NifD and NifK polypeptides were not affected by the Δ*clpX2* mutation (Fig. S4).

The A. vinelandii ΔclpX2 mutant strain exhibits a diazotrophic growth defect that is exacerbated under iron-limiting conditions

The growth of the Δ*clpX2* mutant strain was identical to that of the wild type when using ammonium as nitrogen source. However, the Δ*clpX2* mutant grew slightly slower than the wild type under diazotrophic conditions (Fig. 8A). Consistently, the onset of nitrogenase activity *in vivo* was slower in the Δ*clpX2* mutant than in the wild-type strain (Fig. 8B).

When determined *in vitro* at three hours from derepression, the levels of nitrogenase activity present in cell-free extracts of the wild-type and Δ*clpX2* strains were similar (Table 1).

However, activity measurements of the individual components of nitrogenase showed that Δ*clpX2* cells accumulated 40% more active NifDK component than the wild type while having similar levels of active NifH. No significant difference in apo-NifDK accumulation was evidenced by supplementing the cell free-extracts with purified FeMo-co.

We hypothesized that ClpX2 could confer *A. vinelandii* some advantage during diazotrophic growth under iron-limiting conditions because of the following reasons: (1) the Δ*clpX2* mutant strain exhibited a subtle growth defect during late exponential phase of diazotrophic growth; (2) the levels of NifB and NifEN polypeptides are regulated by ClpX2, both of which are critical proteins for the mobilization of cellular iron towards FeMo-co biosynthesis; and (3) ClpX2 homologs are nutritional-stress associated proteins.

As shown in Fig. 9A, the Δ*clpX2* mutant exhibited slower diazotrophic growth rates than the wild-type strain in medium containing low levels of iron (3 μM). The competitive performance of UW322 (Δ*clpX2*) versus the wild-type strain in different growing conditions is shown in Fig. 9B–C. The Δ*clpX2* strain exhibited a competitive index of 1 when growing using ammonium as nitrogen source and 0.5 when growing diazotrophically. The UW322 competitive index was found to be even lower (0.3) when growing diazotrophically on iron-limited medium. This result supports the idea that ClpX2 confers *A. vinelandii* some advantage during diazotrophic growth, especially under iron limiting conditions.

Discussion

The assembly of active nitrogenase requires a multiplicity of gene products (Fig. 10). While some of them (NifU, NifS, NifB, NifX, NifE, NifN, NifQ, NifH, NifV, NafY and Rnf1) are involved in the biogenesis of either simple or complex [Fe-S] clusters for nitrogenase, others (NifZ, NifW, NafY, NifH and NifM) have roles in the maturation of the nitrogenase polypeptides. The transcription of these genes is coordinately regulated by the NifAL system in response to the presence of ammonium and oxygen (Martinez-Argudo *et al.*, 2004).

The evidence presented in this work demonstrates the existence of another layer of regulation for the FeMo-co biosynthetic pathway in *A. vinelandii*. This regulatory mechanism comprises the proteolytic control of NifB and NifEN levels by a duplicated copy of ClpX that has gained functional specificity (Fig. 10). A proposed mechanism as a working hypothesis for future studies is that a ClpX2-dependent proteolytic pathway might help control the rate of FeMo-co synthesis, and hence nitrogenase activation, according to nutritional and/or environmental stimuli, as proposed here for iron limitation. This might operate to help allocate limiting nutrients to competing branches of metabolism to optimize balanced growth. Several lines of evidence are consistent with this proposal: i) compromised diazotrophic growth under Fe limiting conditions of the *clpX2*-defficient mutant strain, ii) nitrogen source dependent expression of *clpX2*, iii) changes in susceptibility to degradation of NifB ingenetic backgrounds that might change the flux of Fe through NifB (*nifA* and *nifENX*), iv) enhanced "*in vitro*" NifDK activity in *clpX2* mutants. In addition, ClpX2 participation in the biosyntheses of the co-factors of the alternative nitrogenases is apparent through regulation of NifB.

ClpX and ClpP orthologs are found in most bacteria, mitochondria, and chloroplasts. In *E. coli*, ClpP-defective cells show delayed recovery both from stationary phase and following a shift to nutrient poor media. Proteomic analysis of cellular substrates of the ClpXP protease in *E. coli* has revealed five classes of ClpX-recognition signals (Flynn et al., 2003). No obvious matches were found in the *A. vinelandii* NifB, NifE or NifN polypeptides.

Unlike the widespread copy of *clpXP*, the *clpX2* gene is not physically linked to a *clpP* homolog in the *A. vinelandii* chromosome (Setubal et al., 2009). An additional distantly-

related *clpP* homolog (Avin02290) was identified in the genome, raising the question of which one is the protease-component partner of ClpX2 in this bacterium. Tentatively, ClpX2 could be a nitrogen fixation-specific component of a proteolytic complex with ClpP. On the other hand, the *A. vinelandii* genome contains homologs to the *E. coli* adaptor protein SspB, which fine-tunes bacterial stress responses by altering the degradation rates of protein targets by ClpXP, and homologs to the ATP-binding components ClpA and ClpB, as well as the ClpS adaptor protein, which recognizes subsets of specific targets.

Confirming previous mutational analysis (Jacobson *et al.*, 1989), this study shows that *clpX2* is not essential for diazotrophic growth of *A. vinelandii* cultured in Burk's modified medium, indicating that ClpX2 does not play a critical role in nitrogenase assembly or function, as opposed to NifB, NifEN, or NifH. This is in line with the fact that *clpX2* homologs are only present in some diazotrophic bacteria, such as *P. stutzeri*, which is closely related to *A. vinelandii* and carries a *clpX2* gene in an identical genomic environment (*nifM-clpX2-nifF*) (Setubal *et al.*, 2009; Yan *et al.*, 2008).

Microarray analysis of genes expressed under nitrogen-fixing conditions in *P. stutzeri* showed nitrogen source-dependent expression of *clpX2*. The expression of *clpX2* (PST1358) increased 8-fold during nitrogen fixation while decreased to half its value after subjecting diazotrophic cells to an ammonium shock (Yan *et al.*, 2010). Sequence inspection suggested rather distal RpoN and NifA binding motifs in a putative promoter controlling the expression of nine *orfs* (PST1349 to PST1358) in *P. stutzeri*. On the other hand, we show here that in *A. vinelandii* NifA was not required for derepression of *clpX2* expression after ammonium depletion. Future work should address the details of the ammonium-dependent regulation of *A. vinelandii clpX2* expression.

The differential stability of NifB polypeptides in wild type, *nifA* and *nifENX* mutants could indicate the existence of different NifB conformations during the loading and unloading cycle of FeMo-co-precursors, as these conformations might become "frozen" in the different genetic backgrounds. For instance, the instability of GST-NifB in the *nifA* mutant could be due to its inability to induce transcription of other *nif* genes, such as *nifU* and *nifS*, which act as major providers of [Fe-S] cluster substrates for NifB activity (Zhao *et al.*, 2007). On the other hand, inactivation of *nifENX* rendered a GST-NifB protein that was much more resistant to degradation. NifX and NifEN are proteins that bind to the metabolic product of NifB (NifB-co), possibly by interacting with NifB, and are involved in further processing of NifB-co into FeMo-co. The differential susceptibility of NifB to proteolysis in those genetic backgrounds that might alter the flux of FeMo-co precursors through NifB could help understand regulatory aspects of the first committed step in FeMo-co biosynthesis.

Disruption of a house keeping-like copy of *clpX* in *Azospirillum brasilense* resulted in an increased *in vivo* nitrogen-fixation activity among other pleiotropic mutant phenotypes (Rodriguez *et al.*, 2006). The modest rise observed for NifDK nitrogenase-component activity *in vitro* of the *A. vinelandii* Δ*clpX2* mutant strain could be due to enhanced NifB and NifEN activities when they were degraded at a lower rate. However, this increase did not result in higher nitrogen-fixation rates *in vivo*. Moreover, the *A. vinelandii* Δ*clpX2* strain exhibited slightly lower *in vivo* nitrogen-fixation activity and diazotrophic growth rate, which was more noticeable when iron was limiting in the medium.

In *K. pneumoniae*, excess iron has been shown to relieve NifA inhibition by NifL whereas iron depletion abolishes NifA-dependent activation of *nif* genes (Schmitz, 1996). In *A. vinelandii*, iron-dependent regulation of *nif*-gene expression has not been reported yet. In any case, the regulatory mechanism comprising ClpX2-dependent degradation of NifB and

NifEN might operate as a second layer of regulation for a more robust control of the commitment to nitrogen fixation according to the availability of iron.

Identification and characterization of the function of other components involved in the regulatory pathway uncovered in this work will lead to a more detailed understanding of the regulation of nitrogen fixation in *A. vinelandii* and related diazotrophs, which appears to be another important trait regulated by ClpXP proteases.

Experimental procedures

Generation of A. vinelandii mutant strains

A. vinelandii strains UW140 (Δ*nifB*) (Curatti *et al.*, 2006), UW235 (Δ*nifENX*) and UW236 (Hernandez *et al.*, 2007) have been previously described.

To generate strains UW233 and UW238, a DNA fragment comprising the open reading frame of *A. vinelandii nifB* was PCR amplified with the oligonucleotides 5′-GGA TCC ATG GAA CTG AGC GTA CTT GG-3′ and 5′-AAG CTT TCG CTG CCC GCT CAG GCC TTG-3′ and ligated into the *Bam*HI-*Hin*dIII sites of pGEX4T-2 to obtain a *gst::nifB* chimeric gene under the control of the IPTG-inducible tac_P promoter (pRHB148). A *Bgl*II-*Xho*I DNA fragment, comprising the 3′ half of the *A. vinelandii nifB*, the *fdxN* and the *nifO* genes, was obtained from plasmid pRHB13 and used to replace the *Bgl*II-*Xho*I DNA fragment of pRHB148 (comprising the 3′ half of *nifB*) generating pRHB150. Plasmid pRHB150 contains the *lac* repressor gene, *lacI*, for tighter repression of *gst::nifB* expression under non-inducing conditions. This vector was incorporated into the genome of *A. vinelandii* strains UW140 and UW235 by single homologous recombination, generating strains UW233 and UW238, respectively.

To generate strain UW295 (*gst::nifB*, *ΔnifA*), UW233 was transformed with the vector pRHB138, which bears a Δ*nifA::sp* allele (Curatti *et al.*, 2005).

To generate strain UW318, the *lacZ* reporter gene was inserted at a position corresponding to the *clpX2* start codon. Plasmid pRHB295 contains a 1151-bp DNA fragment upstream of *clpX2*, which was amplified from the *A. vinelandii* genome by PCR using oligonucleotides 5′-TTT CGA ATT CCG CGA CGA TGT GAT CGC CAC CCG-3′ and 5′-GTC GGG ATC CTC TCC GCG CCG CAG AAC GAG CAG C-3′, and cloned into the *Eco*RI-*Bam*HI sites of pUC18 (Promega, Madison, WI). Restriction enzymes sites (*Eco*RI and *Bam*HI) incorporated into the oligonucleotides to facilitate vector construction are shown underlined in the oligonucleotide sequences? Plasmid pRHB296 contains a 793-bp DNA fragment downstream of *clpX2* start codon, which was amplified from the *A. vinelandii* genome by PCR with oligonucleotides 5′-ATT GTC TAG ATC CAG CGC CAG GCC GAC GAA CTT-3′ and 5′-GCC GAA GAT GGC AGC GGC CGC ATT CAG CCC GAT C-3′ and cloned into the pGEM-T vector (Promega, Madison, WI). Plasmid pRHB298 contains a 3.1-kb DNA fragment with the *E. coli lacZ* gene amplified by PCR with oligonucleotides 5′-GGA AAC AGC CAT GGC TAA GAT TAC GGA TTC ACT GG-3′ and 5′-AAT ACG GGC AGA CAG CGG CCG CCC GGT TAT TAT TA-3′ and cloned into the pGEM-T vector (Promega, Madison, WI). Plasmid pRHB300 was generated by ligating an *Nco*I-*Xba*I fragment from pRHB295 to an *Nco*I-*Not*I fragment from pRHB298, and a *Not*I-*Xba*I fragment from pRHB296, in order to construct a $clpX2_P$::*lacZ* transcriptional fusion. Positive clones were selected by blue color on X-gal (5-Bromo-4-chloro-3-indolyl-β-D-galactopyranoside) supplemented plates. The fidelity of the construction was confirmed by PCR amplification of the target region using genomic DNA as template. *A. vinelandii* strain UW318 was generated by transformation of wild-type cells with pRHB300, followed by

screening of a blue phenotype on X-gal supplemented plates. Isolated colonies were screened by PCR to confirm the presence and segregation of the *clpX2*$_P$::*lacZ* construction.

A. vinelandii strain UW319 (*clpX2*$_P$::*lacZ*, Δ*nifA::sp*) was generated by transforming UW318 with pRHB138 (Curatti *et al*., 2005). The replacement of *nifA* by the Sp^r cassette in UW139 was confirmed by PCR amplification of the *nifAL* region.

To generate a *clpX2* mutant, an in-frame *clpX2* deletion was introduced into the *A. vinelandii* chromosome. Flanking regions of *clpX2* gene were generated by PCR using the oligonucleotides 5′-TTT CGA ATT CCG CGA CGA TGT GAT CGA CCA CCC G-3′ and 5′-GTC GGG ATC CTC TCC GCG CCG CAG AAC GAG CAG C-3v for the *nifM* region upstream of *clpX2* and 5′-AGC CGG ATC CAT CTC CGG TAG TGG AGG AAA AA-3′ and 5′-ATT GTC TAG ATC CAG CGC CAG GCC GAC GAA CTT-3′ for the *nifF* region downstream of *clpX2*. Restriction enzymes sites (*Eco*RI, *Bam*HI and *Xba*I) incorporated into the oligonucleotides to facilitate vector construction are shown underlined in the oligonucleotide sequences. The resulting products were digested with *Eco*RI-*Bam*HI or *Bam*HI-*Xba*I, respectively, and used in triple-ligation reactions to pUC18, generating plasmid pRHB305, or in quadruple-ligations together with a *Bam*HI-digested kanamycin-resistance cassette to generate pRHB306. Plasmid pRHB306 was introduced into the chromosome of *A. vinelandii* DJ strain by homologous recombination to generate strain UW315. Strain UW322, bearing an in-frame Δ*clpX2* mutation was isolated by cotransforming (congression) strain UW315 with plasmids pRHB305 and pDB303, which contains a rifampicin-resistance marker (kindly provided by D. Dean). Preliminary identification of Δ*clpX2* mutants was verified on rifampicin-containing solid medium by phenotypic loss of kanamycin resistance, which was further confirmed by PCR analysis and sequencing of the locus using genomic DNA of the mutant strains.

All DNA constructions were confirmed by restriction analysis and by DNA sequencing. Generated *A. vinelandii* strains were confirmed by PCR analysis and, when possible, by immunoblot analysis with appropriate antibodies.

Bacterial growth and nitrogenase derepression

E. coli strains were cultivated in Luria-Bertani medium at 37°C with shaking (250 rpm). *A. vinelandii* strains were cultivated in Burk's modified medium at 30°C with modification of the nitrogen or iron sources, when indicated. Antibiotics were added at standard concentrations (Curatti *et al.* 2005). Growth rates were estimated from the light scattering of culture samples at 600 nm using an Ultrospec 3300 pro UV/Visible spectrophotometer (Amersham Biosciences). For the determination of growth curves, ammonium-grown cultures were diluted in fresh ammonium-containing medium to an OD_{600} of 0.5–0.8 and further incubated for 2–3 h. Cells were then collected, washed with and resuspended in ammonium-amended medium, ammonium-free medium, or ammonium-free medium with low iron (3 μM $FeCl_3$) at a final OD_{600} of 0.1. Cells were then incubated at 30°C with shaking (200 rpm).

For nitrogenase derepression, ammonium-grown cells were diluted in fresh ammonium-containing medium to an OD_{600} of 0.5–0.8 and further incubated for 2–3 h. Cells were then collected, washed with and resuspended in ammonium-free medium at a final OD_{600} of 0.75 and incubated at 30°C for 3 h with shaking (200 rpm).

For NifB and NifDK polypeptide turnover experiments shown in Fig. 7 and Fig. S4, cultures were derepressed for nitrogenase during 3 h and then supplemented with 10 $\mu g.ml^{-1}$ spectinomycin to stop protein synthesis, after which samples were collected at different time points.

Note: typically, pulse-chase radiolabeling followed by immuno pull-down is used for studies of *in vivo* degradation of proteins (e.g. Mettert and Kiley, 2005). Because it has been stated that the genus Azotobacter has limited capacity for amino acid transport (Kennedy and Bishop, 2004) these kind of complementary analyses were not attempted in this study.

For *in vivo* loading of *A. vinelandii* cells with GST-NifB, UW233 and UW233-derivative strains were cultivated in ammonium-containing medium and treated with 10 mM IPTG for 2 h. Cells were then collected, washed with medium free of IPTG and further incubated in the media indicated in each *in vivo* NifB-depletion studies.

In vivo and in vitro nitrogenase activities

In vivo nitrogenase activity was determined by the acetylene reduction assay at 30°C for 30 min using 1-ml culture samples as described (Stewart *et al.*, 1967). *In vitro* nitrogenase activity was determined in samples of anaerobic *A. vinelandii* cell-free extracts prepared by osmotic-shock (Shah *et al.*, 1972). Dinitrogenase and dinitrogenase reductase activities were obtained after titration with an excess of the complementary component as described (Shah and Brill, 1973). The specific activity of each protein is defined as nanomoles of ethylene formed per minute per milligram of protein in the extract.

Protein methods

Protein concentration was determined by the bicinchoninic acid method with BSA as the standard (Smith *et al.*, 1985). Procedures for SDS-PAGE (Laemmli, 1970) and immunoblot analysis (Brandner *et al.*, 1989) have been described. Protein samples for immunoblot analyses were prepared by mixing pelleted cells with Laemmli sample buffer 2X. ImageJ software was used to quantify protein levels in immunoblot membranes (Abramoff *et al.*, 2004). β-galactosidase activity was assayed in permeabilized *A. vinelandii* cells following the procedure described by Miller (1972).

Competitive index assays

Competitive index (CI) was defined as the mutant-to-wild-type ratio within the output sample, divided by the corresponding ratio in the inoculum (Macho *et al.*, 2007). For CI assays, a mixed inoculum containing equal CFU of wild-type and mutant strains was inoculated in the indicated Burk's media and incubated at 30°C. Serial dilutions of the mixed cultures were sampled at incubation times 0 (t_0) and 22 h (t_{22}) and plated onto Burk's solid medium (to allow growth of mutant and wild-type strains) and Burk's solid medium supplemented with rifampicin (to inhibit growth of the wild type strain). The t_0 determination was carried out as a control to confirm dose and to obtain the input mutant-to-wild-type ratio. The t_{22} determination was carried out to obtain the output CI values. CI shown are the mean of three independent experiments and the error bars represent standard error.

Supplementary Material

Refer to Web version on PubMed Central for supplementary material.

Acknowledgments

This work is dedicated to the memory of Bob Burris. Authors would like to thank Paul Ludden for his support and valuable discussions and Dennis Dean for calling our attention to *orf9/clpX2* and helpful comments on this research. G. Martínez-Noël and L. Curatti are career researchers at the CONICET, Argentina. This work was supported by National Institute of Health Grant 35332 (to P. Ludden), by ERC Starting Grant 205442 (to L. Rubio), by MICINN BIO2009-12661 Grant (to L. Rubio), by Agencia Nacional de Promoción Científica y Tecnológica Grant PICT 01717 (to L. Curatti), and by Midwestern University Intramural Funds (to J. Hernandez).

References

Abramoff MD, Magelhaes PJ, Ram SJ. Image Processing with ImageJ. Biophotonics International. 2004; 11:36–42.

Bishop PE, Joerger RD. Genetics and molecular biology of alternative nitrogen fixation systems. Annu Rev Plant Physiol Plant Mol Biol. 1990; 41:109–125.

Brandner JP, McEwan AG, Kaplan S, Donohue TJ. Expression of the *Rhodobacter sphaeroides* cytochrome c2 structural gene. J Bacteriol. 1989; 171:360–368. [PubMed: 2536660]

Chan MK, Kim J, Rees DC. The nitrogenase FeMo-cofactor and P-cluster pair: 2.2 A resolution structures. Science. 1993; 260:792–794. [PubMed: 8484118]

Curatti L, Brown CS, Ludden PW, Rubio LM. Genes required for rapid expression of nitrogenase activity in *Azotobacter vinelandii*. Proc Natl Acad Sci USA. 2005; 102:6291–6296. [PubMed: 15845763]

Curatti L, Ludden PW, Rubio LM. NifB-dependent *in vitro* synthesis of the iron-molybdenum cofactor of nitrogenase. Proc Natl Acad Sci USA. 2006; 103:5297–301. [PubMed: 16567617]

Curatti L, Hernandez JA, Igarashi RY, Soboh B, Zhao D, Rubio LM. *In vitro* synthesis of the iron-molybdenum cofactor of nitrogenase from iron, sulfur, molybdenum, and homocitrate using purified proteins. Proc Natl Acad Sci USA. 2007; 104:17626–17631. [PubMed: 17978192]

Dos Santos PC, Johnson DC, Ragle BE, Unciuleac MC, Dean DR. Controlled Expression of nif and isc Iron-Sulfur Protein Maturation Components Reveals Target Specificity and Limited Functional Replacement between the Two Systems. J Bacteriol. 2007; 189:2854–2862. [PubMed: 17237162]

Dougan DA, Mogk A, Zeth K, Turgay K, Bukau B. AAA+ proteins and substrate recognition, it all depends on their partner in crime. FEBS Letters. 2002; 529:6–10. [PubMed: 12354604]

Drummond M, Walmsley J, Kennedy C. Expression from the *nifB* promoter of *Azotobacter vinelandii* can be activated by NifA, VnfA, or AnfA transcriptional activators. J Bacteriol. 1996; 178:788–792. [PubMed: 8550514]

Eady RR. Structure-function relationships of alternative nitrogenases. Chem Rev. 1996; 96:3013–3030. [PubMed: 11848850]

Einsle O, Tezcan FA, Andrade SL, Schmid B, Yoshida M, Howard JB, Rees DC. Nitrogenase MoFe-protein at 1.16 A resolution: a central ligand in the FeMo-cofactor. Science. 2002; 297:1696–1700. [PubMed: 12215645]

Flynn JM, Neher SB, Kim YI, Sauer RT, Baker TA. Proteomic discovery of cellular substrates of the ClpXP protease reveal five classes of ClpX-recognition signals. Mol Cell. 2003; 11:671–683. [PubMed: 12667450]

George SJ, Igarashi RY, Xiao Y, Hernandez JA, Demuez M, Zhao D, Yoda Y, Ludden PW, Rubio LM, Cramer SP. Extended X-ray absorption fine structure and nuclear resonance vibrational Spectroscopy reveal that NifB-co, a FeMo-co precursor, comprises a 6Fe core with an interstitial light atom. J Am Chem Soc. 2008; 130:5673–5680. [PubMed: 18386899]

Hernandez JA, Igarashi RY, Soboh B, Curatti L, Dean DR, Ludden PW, Rubio LM. NifX and NifEN exchange NifB cofactor and the VK-cluster, a newly isolated intermediate of the iron-molybdenum cofactor biosynthetic pathway. Mol Microbiol. 2007; 63:177–192. [PubMed: 17163967]

Jacobson MR, Cash VL, Weiss MC, Laird NF, Newton WE, Dean DR. Biochemical and genetic analysis of the *nifUSVWZM* cluster from *Azotobacter vinelandii*. Mol Gen Genet. 1989; 219:49–57. [PubMed: 2615765]

Kennedy C, Bishop P. Genetics and regulation of nitrogen fixation in free-living bacteria nitrogen fixation: origins, applications, and research progress. Volume. 2004; 2:27–52.

Kim YI, Burton RE, Burton BM, Sauer RT, Baker TA. Dynamics of substrate denaturation and translocation by the ClpXP degradation machine. Mol Cell. 2000; 5:639–648. [PubMed: 10882100]

Laemmli UK. Cleavage of structural proteins during the assembly of the head of bacteriophage T4. Nature. 1970; 227:680–685. [PubMed: 5432063]

Lukoyanov D, Pelmenschikov V, Maeser N, Laryukhin M, Yang TC, Noodleman L, Dean DR, Case DA, Seefeldt LC, Hoffman BM. Testing if the interstitial atom, X, of the nitrogenase

molybdenum-iron cofactor is N or C: ENDOR, ESEEM, and DFT studies of the S = 3/2 resting state in multiple environments. Inorg Chem. 1989; 46:11437–11449. [PubMed: 18027933]

Macho AP, Zumaquero A, Ortiz-Martín I, Beuzón CR. Competitive index in mixed infections: a sensitive and accurate assay for the genetic analysis of Pseudomonas syringae-plant interactions. Mol Plant Path. 2007; 8:437–450. [PubMed: 20507512]

Martinez-Argudo I, Little R, Shearer N, Johnson P, Dixon R. The NifL-NifA System: a Multidomain Transcriptional Regulatory Complex That Integrates Environmental Signals. J Bacteriol. 2004; 186:601–610. [PubMed: 14729684]

Mettert EL, Kiley PJ. ClpXP-dependent proteolysis of FNR upon loss of its O_2-sensing [4Fe–4S] cluster. J Mol Biol. 2005; 354:220–232. [PubMed: 16243354]

Miller, JH. Experiments in Molecular Genetics. Cold Spring Harbor Lab. Press; Plainview, NY: 1972.

Rodriguez H, Mendoza A, Cruz MA, Holguin G, Glick BR, Bashan Y. Pleiotropic physiological effects in the plant growth-promoting bacterium *Azospirillum brasilense* following chromosomal labeling in the *clpX* gene. FEMS Microbiol Ecol. 2006; 57:217–225. [PubMed: 16867140]

Rubio LM, Ludden PW. Biosynthesis of the iron-molybdenum cofactor of nitrogenase. Annu Rev Microbiol. 2008; 62:93–111. [PubMed: 18429691]

Setubal JC, Dos Santos P, Goldman BS, Ertesvåg H, Espin G, Rubio LM, et al. Genome sequence of *Azotobacter vinelandii*, an obligate aerobe specialized to support diverse anaerobic metabolic processes. J Bacteriol. 2009; 191:4534–4545. [PubMed: 19429624]

Schmitz RA, He L, Kustu S. Iron is required to relieve inhibitory effects on NifL on transcriptional activation by NifA in *Klebsiella pneumoniae*. J Bacteriol. 1996; 178:4679–4687. [PubMed: 8755900]

Shah VK, Allen JR, Spangler NJ, Ludden PW. *In vitro* synthesis of the iron-molybdenum cofactor of nitrogenase. Purification and characterization of NifB cofactor, the product of NIFB protein. J Biol Chem. 1994; 269:1154–1158. [PubMed: 8288575]

Shah VK, Davis LC, Brill WJ. Nitrogenase. I. Repression and derepression of the iron-molybdenum and iron proteins of nitrogenase in *Azotobacter vinelandii*. Biochim Biophys Acta. 1972; 256:498–511. [PubMed: 5016550]

Shah VK, Brill WJ. Nitrogenase. IV. Simple method of purification to homogeneity of nitrogenase components from *Azotobacter vinelandii*. Biochim Biophys Acta. 1973; 305:445–454. [PubMed: 4354875]

Smith PK, Krohn RI, Hermanson GT, Mallia AK, Gartner FH, Provenzano MD, et al. Measurement of protein using bicinchoninic acid. Anal Biochem. 1985; 150:76–85. [PubMed: 3843705]

Stewart WDP, Fitzgerald GP, Burris RH. *In situ* studies on N_2 fixation using the acetylene reduction technique. Proc Natl Acad Sci USA. 1967; 58:2071–2078. [PubMed: 5237501]

Yan Y, Yang J, Dou Y, Chen M, Ping S, Peng J, et al. Nitrogen fixation island and rhizosphere competence traits in the genome of root-associated *Pseudomonas stutzeri* A1501. Proc Natl Acad Sci USA. 2008; 105:7564–7569. [PubMed: 18495935]

Yan Y, Ping S, Peng J, Han Y, Li L, Yang J, et al. Global transcriptional analysis of nitrogen fixation and ammonium repression in root-associated *Pseudomonas stutzeri* A1501. BMC Genomics. 2010; 11:11–24. [PubMed: 20053297]

Zhao D, Curatti L, Rubio LM. Evidence for *nifU* and *nifS* participation in the biosynthesis of the iron-molybdenum cofactor of nitrogenase. J Biol Chem. 2007; 282:37016–37025. [PubMed: 17959596]

Zolkiewski M. A camel passes through the eye of a needle: protein unfolding activity of Clp ATPases. Mol Microbiol. 2006; 61:1094–1100. [PubMed: 16879409]

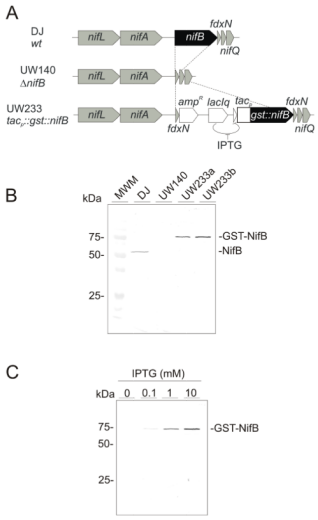

Fig. 1.

Artificially controlled expression of NifB in *A. vinelandii*. A, comparison of physical maps of *A. vinelandii* chromosomal regions around the *nifB* locus in the wild-type strain (DJ), a Δ*nifB* strain (UW140), and an IPTG-controlled *gst::nifB*-expressing strain (UW233). B, Immunoblot developed with antibodies to NifB showing accumulation of NifB or GST-NifB in *A. vinelandii* strains, DJ, UW140 and two clones of strain UW233. All strains were derepressed for nitrogen fixation during 4 h; in addition, UW233 cultures were treated with 1 mM IPTG. C, GST-NifB accumulation in strain UW233 under nitrogenase derepressing conditions in medium supplemented with increasing concentrations of IPTG.

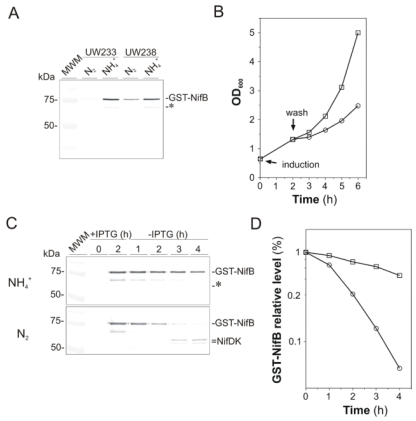

Fig. 2.

Differential degradation of GST-NifB under diazotrophic and non-diazotrophic growing conditions. A, Immunoblot analysis showing the IPTG-induced accumulation of GST-NifB in cells of *A. vinelandii* UW233 and UW238 strains growing under ammonium- or N_2-dependent conditions. UW238 is a Δ*nifENX::kn* derivative of UW233. B, Growth curves of UW233 cells loaded with GST-NifB by IPTG induction in medium containing ammonium and then transferred to diazotrophic (circles) or ammonium-containing (squares) medium lacking IPTG. C, Degradation profile of GST-NifB protein accumulated in UW233 cells treated as described in B. For this analysis, the immunoblot was developed with a mixture of anti-NifB and anti-NifDK antibodies. The asterisk points to a GST-NifB-degradation product. D, Densitometric quantitation of GST-NifB disappearance under ammonium-dependent (squares) or diazotrophic (circles) growing conditions. This representative plot was generated by using the GST-NifB immunoblot shown in C.

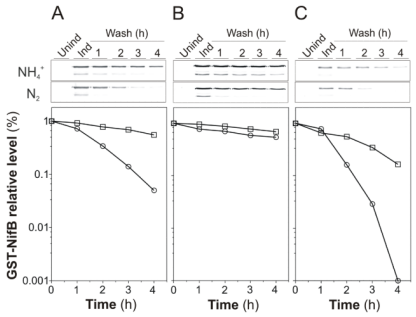

Fig. 3.

Effect of Δ*nifENX* and Δ*nifA* mutations on the degradation rates of GST-NifB protein. Immunoblot analyses of GST-NifB accumulated under diazotrophic or ammonium-amended medium in *A. vinelandii* strains UW233 (A), UW238 (B), and UW295 (C). UW238 is a Δ*nifENX::kn* derivative of UW233. UW295 is a Δ*nifA::sp* derivative of UW233. *A. vinelandii* cells cultured in medium containing ammonium (Unind) were induced for GST-NifB expression during 2 h by adding IPTG to the medium (Ind). Cells were then treated as described in Fig. 2B and analyzed by immunoblot developed with antibodies to NifB. The asterisk points to a GST-NifB-degradation product. Densitometric quantitations of GST-NifB disappearance under ammonium-dependent (squares) or diazotrophic (circles) growing conditions are shown for each strain.

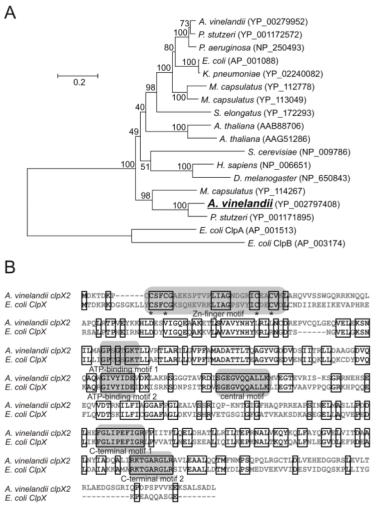

Fig. 4.

A. vinelandii ClpX2 sequence analysis. A, Neighbour joining phylogenetic tree of the *A. vinelandii* ClpX2 polypeptide (shown in bold). Sequence data used to generate the tree were obtained from the NCBI nr database. Numbers adjacent to each node show the bootstrap percentage. B, Sequence alignment of the *A. vinelandii* ClpX2 and *Escherichia coli* ClpX polypeptides showing conservation of domains known to be relevant to *E. coli* ClpX function.

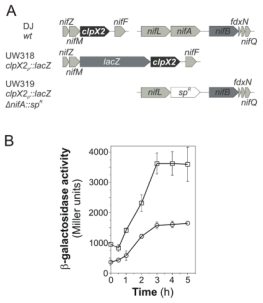

Fig. 5.

A. vinelandii clpX2 expression. A, physical map of the *clpX2* locus in *A. vinelandii* strains DJ, UW318 and UW319. B, β-galactosidase activity following ammonium step-down in strains UW318 (open circles) and UW319 (open squares). Ammonium was removed from the medium at time zero.

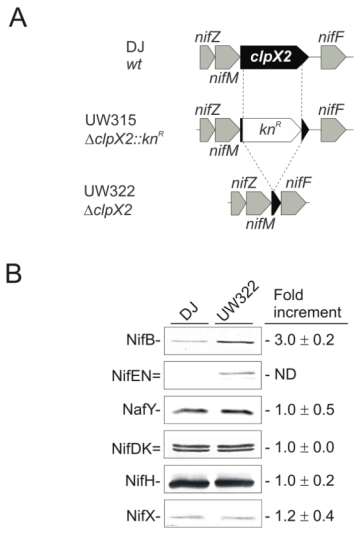

Fig. 6.

Accumulation of Nif proteins in wild-type and *clpX2* strains. A, Genetic map of *A. vinelandii clpX2* region in the wild-type and the *clpX2* strains. B, Immunoblot analyses of NifB, NifEN, NafY, NifDK, NifH and NifX proteins in cell-free extracts of wild-type and *clpX2* mutant strains under nitrogenase-derepressing conditions. Representative immunoblots are shown. Changes in protein accumulation were estimated by densitometric quantification of immunoblots using the ImageJ software. Values are the mean and standard deviations of at least two independent experiments. N.D. means not determined due to the very low levels of NifEN in extracts of DJ strain.

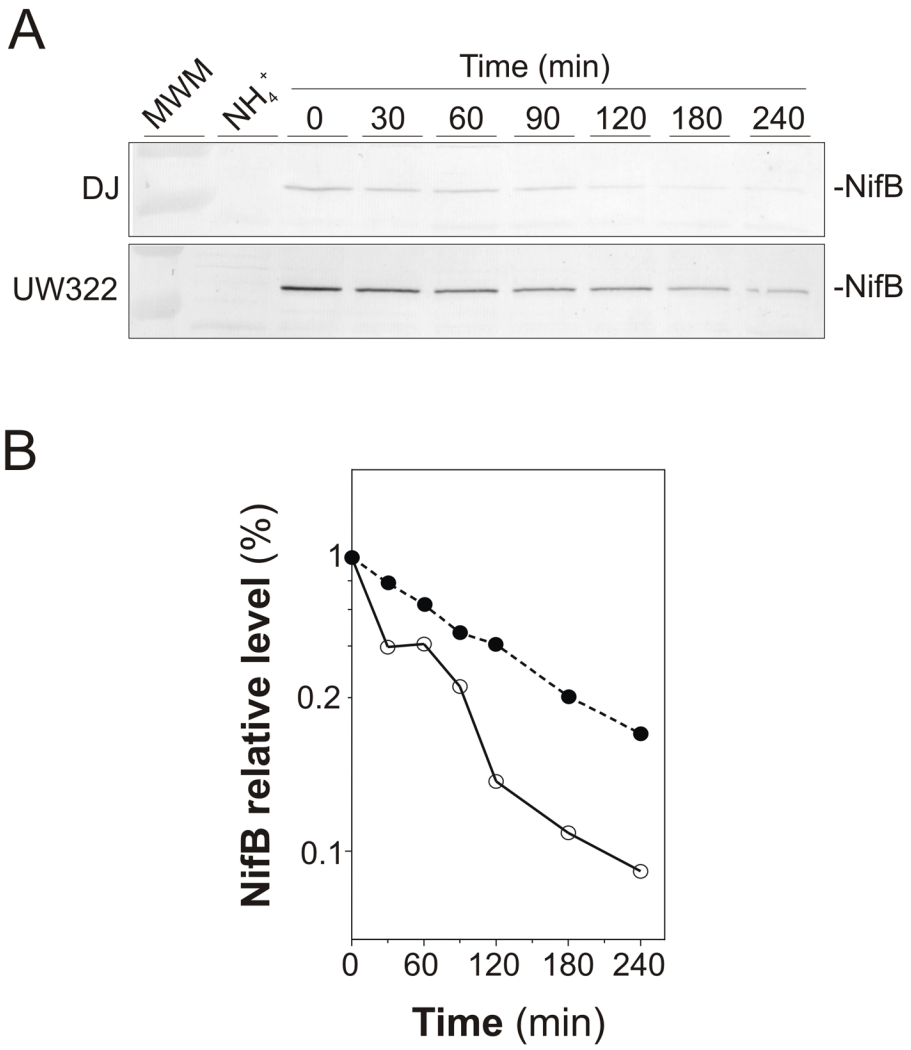

Fig. 7.

Degradation of NifB polypeptide over time in the wild-type and the *clpX2* strains. A, Time-course analysis of NifB protein accumulation in cell-free extracts from wild-type (DJ) and *clpX2* strains derepressed for nitrogenase and treated with spectinomycin (10 μg.ml^{-1}) to stop protein synthesis. Cell-free extracts obtained from cells grown with ammonium were used as controls. Immunoblots were developed with antibodies to NifB. A representative immunoblot is shown. B, Relative NifB levels in the wild-type (open circles) and the *clpX2* (closed circles) strains estimated by densitometric quantification of immunoblots shown in A.

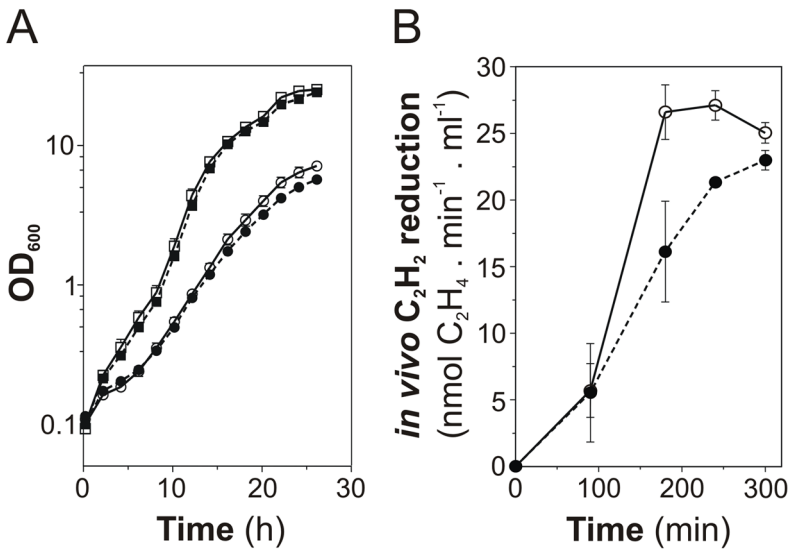

Fig. 8.

Effect of deleting *A. vinelandii clpX2* on diazotrophic growth and *in vivo* nitrogen fixation. A, Growth curves of *A. vinelandii* strains DJ (open symbols) and UW322 (closed symbols) using ammonium (squares) or N_2 (circles) as nitrogen source. B, Time-course development of *in vivo* nitrogen fixation activity in *A. vinelandii* strains DJ (open symbols) and UW322 (closed symbols) estimated by the acetylene reduction assay. Data represent the mean and standard deviation of three independent experiments.

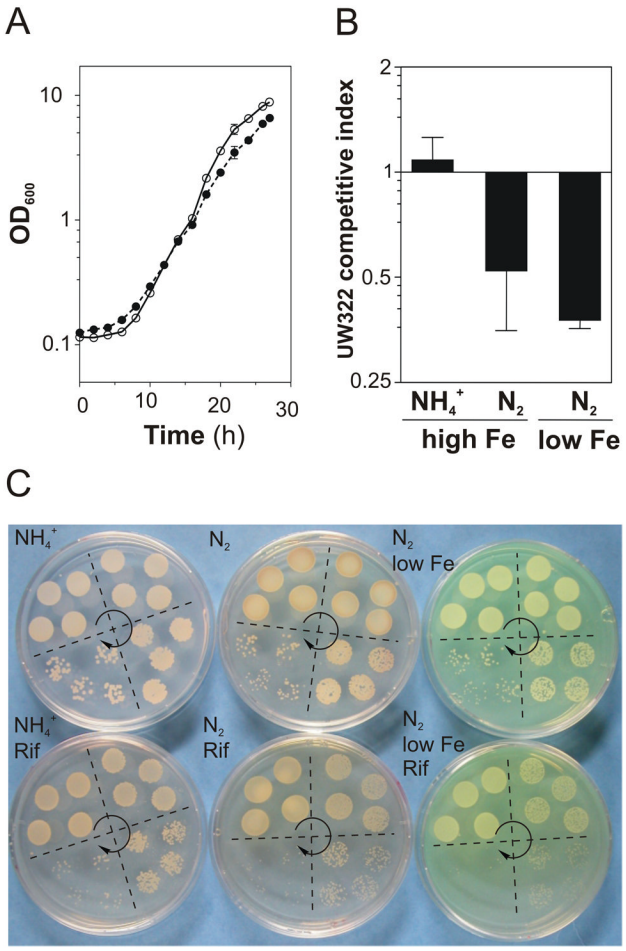

Fig. 9.

Effect of deleting *A. vinelandii clpX2* on diazotrophic growth under iron limiting conditions. A, Growth curves of *A. vinelandii* DJ (open symbols) and UW322 (closed symbols) under low-iron nitrogenase-derepressing conditions. B, Effect of diazotrophy and iron supply on the competitive index of UW322. Competitive indexes were obtained from mixed cultures (1:1 ratio) of DJ and UW322 strains. Data represent the mean and standard deviation of three independent experiments. C, Representative plates showing the development on solid medium of mixed cultures that were pre-grown in liquid medium for 22 h before plating. Four equivalent drops at different dilutions (10^{-3}, 10^{-4}, 10^{-5} or 10^{-6}) of DJ and UW322 mixed cultures were plated on each quarter of the plates. Arrows show the direction of the dilutions. Cells were inoculated on media lacking rifampicin (to allow DJ and UW322 growth) and media supplemented with rifampicin (to allow only UW322 growth). Competitive growth was tested in ammonium-containing medium, ammonium-lacking medium, and low-iron (3 μM) ammonium-lacking medium.

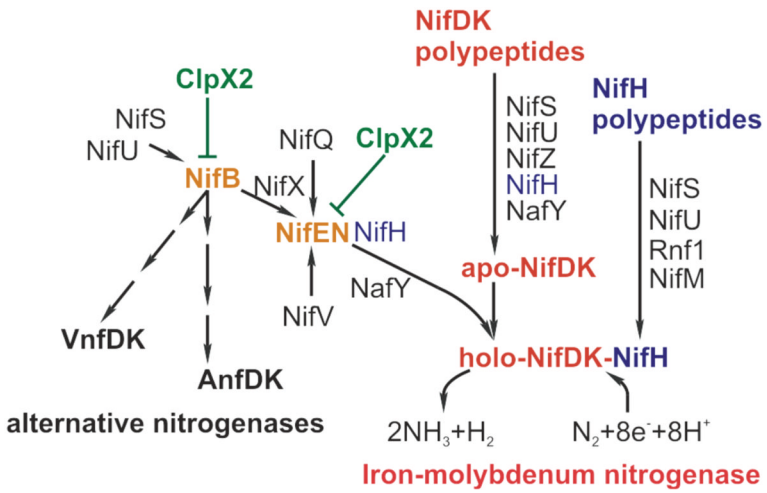

Fig. 10.

Diagram of Nif-proteins participation in the formation of active nitrogenase in *A. vinelandii*. The function of Nif proteins has been reviewed recently (Rubio and Ludden, 2008). Color code: red, NifDK polypeptides; blue, NifH polypeptides; green, ClpX2; yellow, ClpX2 targets; black, other proteins involved in nitrogenase assembly.

Table 1

Comparison of *in vitro* nitrogenase-component activities between the wild-type and the Δ*clpX2* strains[1]

	DJ (*wt*)	UW322 (*clpX2*)
Nitrogenase	40,62 ± 9,47	46,09 ± 12,13
Dinitrogenase[2]	108,92 ± 17,67	151,89 ± 21,50
Dinitrogenase reductase[3]	50,88 ± 1,26	58,04 ± 7,32
FeMo-co[4]	37,05 ± 14,52	46,09 ± 7,31

[1] nmol C_2H_4.min^{-1}.mg $protein^{-1}$

[2] assayed in the presence of an excess of purified dinitrogenase reductase (NifH)

[3] assayed in the presence of an excess of purified dinitrogenase (NifDK)

[4] assayed in the presence of an excess of purified FeMo-co